Chapter 2
Fundamentals of Defect Ionization and Transport

2.1 Introduction

Native atomic defects include vacancies, interstitials, and antisite defects. Antisite defects, which consist of atoms residing in improper lattice sites, are relevant only for binary compounds such as III–V or oxide semiconductors. One such example is a gallium atom occupying an arsenic atom lattice site, denoted as Ga_{As}, rather that its proper gallium atom lattice site. Defect clusters or complexes are formed when two or more of the atomic defects mentioned above join together. Examples of clusters include divacancies, trivacancies, di-interstitials, vacancy-interstitial pairs, etc. Clusters on the surface may be referred to as vacancy or adatom islands. The basic defect thermodynamics are the same for the bulk and surface. For an explicit discussion of the correspondence in defect structure and behavior between the two, the reader should refer to Table 5.2 in Chap. 5. In addition to native or intrinsic defects, extrinsic defects may also exist in the crystal lattice. These defects formed either intentionally (via doping or ion implantation, for instance) or accidentally by the introduction of foreign atoms into the semiconductor. In boron-doped silicon, for example, the two most likely extrinsic defects are boron in a silicon lattice site, donated as B_{Si}, and boron in an interstitial location, B_i.

2.2 Thermodynamics of Defect Charging

The thermodynamics of defect charging have been discussed in numerous journal articles and books (Van Vechten 1980; Van Vechten and Thurmond 1976b, a; Fahey *et al.* 1989; Pichler 2004; Jarzebski 1973). Note that the thermodynamic parameters, including band gaps, ionization energies, and energies of defect formation and/or migration, are not the eigenvalues of a Schrodinger equation describing the crystal (Van Vechten 1980). The thermodynamic parameters are defined statistically in terms of reactions occurring among ensembles of all possible configurations of the

E.G. Seebauer, M.C. Kratzer, *Charged Semiconductor Defects*,

system. Confusion over this distinction sometimes exists particularly with reference to ionization levels.

When thermally generated or artificial point defects are introduced into a perfect semiconductor crystal, they increase the Gibbs free energy G of the system. The equilibrium concentration [X] of a neutral point defect X^0 can be expressed as

$$\frac{\left[X^0\right]}{\left[S\right]} = \theta_{X^0} \exp\left[\frac{-G^f_{X^0}}{kT}\right] = \theta_{X^0} \exp\left[\frac{S^f_{X^0}}{k}\right] \exp\left[\frac{-H^f_{X^0}}{kT}\right] \tag{2.1}$$

where [S] is the concentration of available lattice sites in the crystal, θ_{X^0} is the number of degrees of internal freedom of the defect on a lattice site, and $G^f_{X^0}$, $H^f_{X^0}$, and $S^f_{X^0}$ are respectively the standard Gibbs free energy, enthalpy, and entropy of neutral defect formation (Fahey *et al.* 1989; Bourgoin and Lannoo 1981; Swalin 1962). The parameters k and T respectively represent Boltzmann's constant and temperature. A defect may have several degrees of freedom due to spin degeneracy or equivalent geometric configurations at the same site (Pichler 2004). Typically only the spin degeneracy is of direct interest for defect charging. For simplicity, therefore, the discussion henceforth will focus upon the spin-degeneracy g rather than other degrees of internal freedom of the defect.

In the case that two identical defects bind together to form a defect pair or complex, the concentration of the combined defect X_2 is given by

$$\left[X_2\right] = \theta_{X_2} \frac{\left[X\right]\left[X\right]}{\left[S\right]} \exp\left[\frac{E^b_{X_2}}{kT}\right] \tag{2.2}$$

where $E^b_{X_2}$ denotes the binding energy of the X_2 defect, and the degeneracy factor θ_{X_2} equals the number of equivalent ways of forming the X_2 defect at a particular site (Fahey *et al.* 1989). The thermodynamics of defect clustering will be discussed in greater detail in Sect. 2.1.3.

For oxide semiconductors, which typically exhibit small deviations from stoichiometry on the order of a few parts per thousand, it is possible to rewrite Eq. 2.1 to explicitly reflect the dependence of [X] upon the ambient oxygen pressure P_{O_2}. However, it becomes necessary to incorporate several additional variables including $[M_M]$, the concentration of metal in the metal sublattice, and $[O_O]$, the concentration of oxygen in the oxygen sublattice (Jarzebski 1973). It then follows that the concentration of vacancies in the metal sublattice is given by the mass-action expression

$$\frac{\left[V_M\right]}{\left[M_M\right]} = P_M^{-\alpha} \exp\left[\frac{\Delta S_1}{k}\right] \exp\left[-\frac{\Delta H_1}{kT}\right] \tag{2.3}$$

and that of vacancies in the oxygen sublattice by

$$\frac{\left[V_O\right]}{\left[O_O\right]} = P_{O_2}^{-\alpha} \exp\left[\frac{\Delta S_2 - \Delta S_1}{k}\right] \exp\left[-\frac{\Delta H_2 - \Delta H_1}{kT}\right] \tag{2.4}$$

where the constant α derives from the ratio of oxygen to metal in the MO or MO_2 crystal (Jarzebski 1973). For instance, α theoretically equals ½ for a perfectly stoichiometric oxide semiconductor of type MO. Generally α takes the form $\alpha = 1/n$, where n is an integer. n must always be an integer in order to preserve bulk charge neutrality. Values for n ranging anywhere from 2–8 appear in the literature. As the stoichiometry of most oxide semiconductors is highly temperature dependent, the empirical values of n are typically determined from temperature-dependent electrical conductivity measurements. ΔS_1 and ΔS_2 may contain contributions from the vibrational entropy of the crystal resulting from the addition of V_M, V_O, and extra oxygen atoms, as well as the standard Gibbs free entropy of the oxygen molecule in the gas phase $\Delta S^{\circ}_{O_2}$. The ΔH parameters contain the enthalpies associated with the same defect processes (Jarzebski 1973).

For neutral defects, the equilibrium concentration of point defects does not depend upon the value of the chemical potential (or more colloquially, "Fermi energy" $E_{F,}$ even for $T > 0$ K) in the bulk. This is not the case for charged defects.

2.2.1 *Free Energies, Ionization Levels, and Charged Defect Concentrations*

Neutral defects almost always have unsaturated bonding capabilities (*e.g.*, dangling bonds). These capabilities facilitate the transfer of electronic charge between the host matrix and the defect, and often occur to the point that the defect becomes fully ionized. The degree and direction of electron transfer (toward or away from the defect, respectively, for acceptors and donors) naturally depend upon the electron richness of the host, as quantified by the host's Fermi energy (*i.e.*, chemical potential) in the vicinity of the defect. In semiconductors, the host's electron richness can be adjusted readily by doping, imposed electric fields, photostimulation, and other factors. Thus, the ionization state of the defect can often be controlled. If the defect possesses significant capacity to store excess charge within its structure, the range of ionization states can be quite large. For example, a monovacancy in silicon nominally incorporates four unsaturated dangling bonds, and permits charge states ranging from (–2) to (+2) (Fahey *et al.* 1989; Schultz 2006).

Some defects have eigenstates close to the edges of the valence band or conduction band; these states can be described by a hydrogenic model with a ground state and a series of bound excited states described by hydrogen atom wavefunctions, with full ionization occurring into the energy continuum of the valence or conduction band. This simple picture must, of course, be modified to account for the interactions of the electrons and holes with the lattice, which alters their effective mass. Also, the crystal reduces the binding potential, which incorporates a dielectric constant (Queisser and Haller 1998). For defects having eigenstates deeper within the band gap of the semiconductor, a more detailed quantum mechanical treatment is needed.

For many purposes, the concentration of defects in a given charge state must be known. This concentration requires use of Fermi statistics, whose application to semiconductors is reviewed briefly here. Electrons in solids obey Fermi–Dirac statistics, for which the distribution of electrons over a range of allowed energy levels at thermal equilibrium is

$$f(E) = \frac{1}{1 + e^{(E - E_F)/kT}} \tag{2.5}$$

where k is again Boltzmann's constant, $f(E)$ the probability that an available energy state at E will be occupied by an electron at absolute temperature T. The physical interpretation of the chemical potential E_F is that the probability of electron occupation is exactly 0.5 in an energy state lying at E_F. In the limit of zero temperature, the chemical potential equals the Fermi energy. Although the Fermi energy is a concept that has formal meaning only in this limit, colloquial terminology commonly uses "chemical potential" and "Fermi energy" interchangeably at all temperatures, and the present treatment will follow that practice.

In an ideal intrinsic (undoped) semiconductor, the Fermi energy E_F takes the value

$$E_F = \frac{E_C + E_V}{2} + \frac{kT}{2} \ln \frac{N_V}{N_C} \tag{2.6}$$

where E_C is the energy at the bottom of the conduction band, E_V is the energy at the top of the valence band, and $N_V (N_C)$ is the effective density of states in the valence (conduction) band. For intrinsic material, the Fermi level lies approximately in the middle of the band gap.

The product of the two charge-carrier concentrations is independent of the Fermi level and obeys

$$n_i^2 = p_i^2 = n \cdot p \tag{2.7}$$

where $n_i (p_i)$ is the intrinsic concentration of electrons (holes). Clearly, in undoped material, the concentrations of electrons and holes are equal. For reference, the intrinsic concentration for Si at room temperature is approximately $1.5 \times 10^{10}\ \mathrm{cm}^{-3}$.

In doped material, the electron and hole concentrations are no longer identical. Boltzmann statistics can be used under most conditions to approximate Fermi statistics and obtain a probability that a state is occupied by an electron. The electron and hole concentrations can also be approximated by:

$$n = N_C \exp\left(\frac{E_F - E_C}{kT}\right) \tag{2.8}$$

and

$$p = N_V \exp\left(\frac{E_V - E_F}{kT}\right) \tag{2.9}$$

with parameters identical to those in Eq. 2.6. When n and p are varied by doping, the Fermi level either rises toward the conduction band (made more n-type) or falls toward the valence band (made more p-type). This variation in Fermi energy must be taken into account when calculating the concentration of charged defects in the bulk.

Fermi–Dirac statistics apply to the calculation of charged defect concentrations as follows. Take, for instance, the ionization of an acceptor defect X to X^{-1}, which can be represented by the reaction:

$$X^0 \leftrightarrow X^{-1} + h^{+1}. \tag{2.10}$$

Equation 2.10 is equally valid for point defects such as vacancies and self-interstitials as it is for divacancies and substitutional extrinsic defects. The law of mass action implies that

$$\left[X^{-1}\right] = \frac{[X]}{1 + g\left(X^{-1}\right)\exp\left[\dfrac{E_{X^{-1}} - E_F}{kT}\right]}, \tag{2.11}$$

where [X] is the concentration of the defect in all charge states, g is an overall degeneracy factor, and $E_{X^{-1}}$ is the ionization level for the singly ionized acceptor. This expression can be simplified when $\left|E_{X^{-1}} - E_F\right| >> \mathrm{kT}$. Also, in the case that defect X has only two charge states, g is simply the ratio of the degeneracy of X^{-1} to that of X^0, as shown in Eq. 2.12:

$$\frac{\left[X^{-1}\right]}{\left[X^0\right]} = \frac{\theta_{X^{-1}}}{\theta_{X^0}}\exp\left[\frac{E_F - E_{X^{-1}}}{kT}\right], \tag{2.12}$$

where $\theta_{X^{-1}}$ and θ_{X^0} respectively denote degeneracy factors for X^{-1} and X^0.

In the same way, the single ionization of a donor defect can be represented by the reaction

$$X^0 \leftrightarrow X^{+1} + e^{-1}, \tag{2.13}$$

where the concentration of X^{+1} can be determined from Eq. 2.14:

$$\left[X^{+1}\right] = \frac{[X]}{1 + g\left(X^{+1}\right)\exp\left[\dfrac{E_F - E_{X^{+1}}}{kT}\right]} \tag{2.14}$$

or Eq. 2.15, when $\left|\mathrm{E_F} - E_{X^{+1}}\right| >> kT$:

$$\frac{\left[X^{+1}\right]}{\left[X^0\right]} = \frac{\theta_{X^{+1}}}{\theta_{X^0}}\exp\left[\frac{E_{X^{+1}} - E_F}{kT}\right]. \tag{2.15}$$

The ionization levels in Eqs. 2.11 and 2.14 do not represent the eigenvalues of a Schroedinger equation, but rather thermodynamic quantities based on occupation

statistics. In particular, the ionization level equals the value of the Fermi energy at which the concentrations of the two charge states are identical (to within a degeneracy factor). For example, if $\theta_{X^{-1}} = \theta_{X^0}$ in Eq. 2.12, then $[X^{-1}] = [X^0]$ when $E_F = E_{X^{-1}}$.

The degeneracy factors in Eqs. 2.11 and 2.14 are usually concerned with differences in net electron spin among the charge states. For both acceptor and donor defects, the value of the overall degeneracy factor g can be deduced by applying the principle of equal occupation of states when E_F is equal to the ionization level under consideration. As an example, neutral vacancy defects have no spin degeneracy, as they have no bound carriers. However, if one additional singly charged state exists (either X^{+1} or X^{-1}), that singly charged state is twofold spin degenerate with electron spins that can be either up or down. Thus, for the specific case of a positive vacancy, we must have $[V^{+1}] = 2[V^0]$ or alternatively $[V^{+1}] = 2/3\ [V^0]$, so $g(V^{+1}) = ½$. The same argument gives $g(V^{-1}) = ½$.

Analogs of Eqs. 2.12 and 2.15 for charge states of two or higher can be constructed by induction from the single charge states. As an example, the concentration of the multiply charged acceptor X^{-2} with ionization level $E_{X^{-2}}$ is:

$$\frac{\left[X^{-2}\right]}{\left[X^0\right]} = \frac{\theta_{X^{-2}}}{\theta_{X^0}} \exp\left[-\frac{E_{X^{-2}} + E_{X^{-1}} - 2E_F}{kT}\right], \tag{2.16}$$

while that of the doubly ionized donor X^{+2} is:

$$\frac{\left[X^{+2}\right]}{\left[X^0\right]} = \frac{\theta_{X^{+2}}}{\theta_{X^0}} \exp\left[-\frac{2E_F - E_{X^{+2}} - E_{X^{+1}}}{kT}\right]. \tag{2.17}$$

Clearly the charged defect concentrations vary with T. Figure 2.1 shows the concentration of charged vacancies in silicon at 300 and 1,400 K as determined by Van Vechten and Thurmond (1976b).

The fact that the concentration of a charged defect depends upon its charge state and the position of the Fermi energy implies related dependencies in the defect's formation energy. After all, there is work involved in moving an electron from the Fermi energy into the energy state associated with the defect. At first glance, the formation of X^{-1} can be written as

$$G^f_{X^{-1}} = G^f_{X^0} + E_{X^{-1}} \tag{2.18}$$

where $G^f_{X^0} = H^f_{X^0} - TS^f_{X^0}$ (Fahey *et al.* 1989). However, this expression neglects the fact that for each ionized defect, an appropriate number of charge carriers are generated. Thus, it is more accurate to generalize the formation energy of the charged defect to

$$G^f_{X^q + e^{-q}} = G^f_{X^q} - qE_F, \tag{2.19}$$

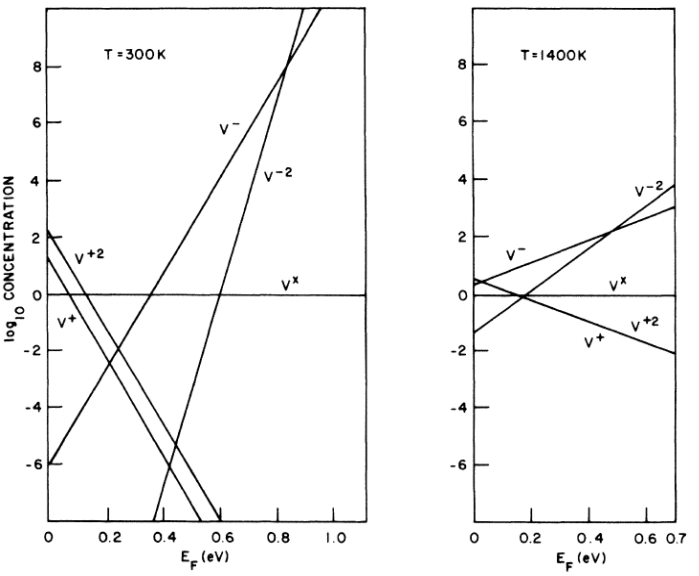

Fig. 2.1 Variation with E_F of the concentration of various vacancy charge states in silicon relative to the neutral. The majority species change with temperature. For example, the neutral state exists at 300 K for E_F between $E_v + 0.14$ eV (ionization level for (+2/0)) and $E_v + 0.35$ eV (ionization level for (0/−1)). However, at 1,400 K only the neutral vacancy is never the majority charge state. Note that a smaller range of E_F is shown for 1,400 K than for 300 K because of band gap narrowing with increasing temperature. Reprinted figure with permission from Van Vechten, JA (1986) Phys Rev B: Condens Matter 33: 2678. Copyright (1986) by the American Physical Society.

where q is the charge state of defect X and E_F is the Fermi energy. When considering a surface defect as opposed to a bulk defect, all the same basic principles apply except that the value of the Fermi energy at the surface (which often differs from that in the bulk) determines the concentrations of various ionization states.

For practical purposes, it is often more useful to examine the work (or Gibbs free energy) associated with ionizing the defect. For the case of X^{-1} the change in free energy associated with ionization, Eq. 2.19, can be rearranged and combined with Eq. 2.18 to yield

$$\Delta G^f_{X^{-1}} = G^f_{X^{-1}} - G^f_{X^0} = E_{X^{-1}} - E_F. \tag{2.20}$$

The origin of Eq. 2.11 should now be explicitly clear. The corresponding free energy of ionization for the doubly ionized acceptor and singly ionized donor are given by

$$\Delta G^f_{X^{-2}} = G^f_{X^{-2}} - G^f_{X^0} = E_{X^{-2}} + E_{X^{-1}} - 2E_F \tag{2.21}$$

and

$$\Delta G^f_{X^{+1}} = G^f_{X^{+1}} - G^f_{X^0} = E_F - E_{X^{+1}}. \tag{2.22}$$

These free energies of defect ionization can be decomposed into corresponding enthalpies and entropies of ionization, $\Delta H^f_{X^q}$ and $\Delta S^f_{X^q}$:

$$\Delta G^f_{X^q} = \Delta H^f_{X^q} - T\Delta S^f_{X^q}. \tag{2.23}$$

Note that $\Delta G^f_{X^q}$, $\Delta H^f_{X^q}$, and $\Delta S^f_{X^q}$ all depend on temperature. The enthalpy of ionization is strongly affected by the degree of localization of the remaining bound carrier of the ionized state. A greater value of $\Delta H^f_{X^q}$ corresponds to an ionization level deeper within the band gap and a remaining carrier that is more loosely bound to the defect center. The value of $\Delta H^f_{X^q}$ at non-zero temperatures can be obtained from an empirical expression due to Varshni (1967) for the band gap energy E_g (equivalent to the free energy of electron-hole pair formation):

$$E_g(T) = E_g(0) - \frac{\alpha T^2}{(T+\beta)} \tag{2.24}$$

where α and β are empirical constants. Since E_g is the increase in free energy, ΔG_{cv}, when an electron-hole pair is created, its temperature derivative is the negative standard entropy of that reaction (Van Vechten 1980),

$$\frac{\partial E_g}{\partial T} \equiv -\Delta S_{cv}. \tag{2.25}$$

Then the definition ΔG = ΔH – TΔS implies

$$\Delta H_{cv}(T) = E_g(T) - T\frac{\partial E_g(T)}{\partial T} \tag{2.26}$$

where ΔH_{cv} is the enthalpy of electron-hole pair formation. Substitution of the derivative of Eq. 2.24 into the expression above yields the following empirical expression for enthalpy of electron-hole pair formation at non-zero temperatures:

$$\Delta H_{cv}(T) = E_g(0) + \frac{\alpha\beta T^2}{(T+\beta)^2}. \tag{2.27}$$

As an example, for Si the relevant constants are $\alpha = 0.000473$ eV/K, $E_g(0) = 1.17$ eV and $\beta = 636$ K (Thurmond 1975). The enthalpy of ionization obtained from Eq. 2.25, when combined with $\Delta H^f_{X^q}$ at $T = 0$ K as deduced from experiment or DFT calculations (as ΔG_{cv} at 0 K equals ΔH_{cv}) (Dev and Seebauer 2003), is then used to describe the variation in enthalpy as a function of charge state according to

$$\Delta H^f_{X^q}(T) = \Delta H^f_{X^q}(0) + \Delta H_{cv}(T). \tag{2.28}$$

The enthalpy of ionization at 0 K, $\Delta H^f_{X^q}(0)$, is charge state-dependent, thus the enthalpies of multiply charged defects phenomenologically track with each other as a function of temperature, yet have different maxima and minima, as shown in Fig. 2.2.

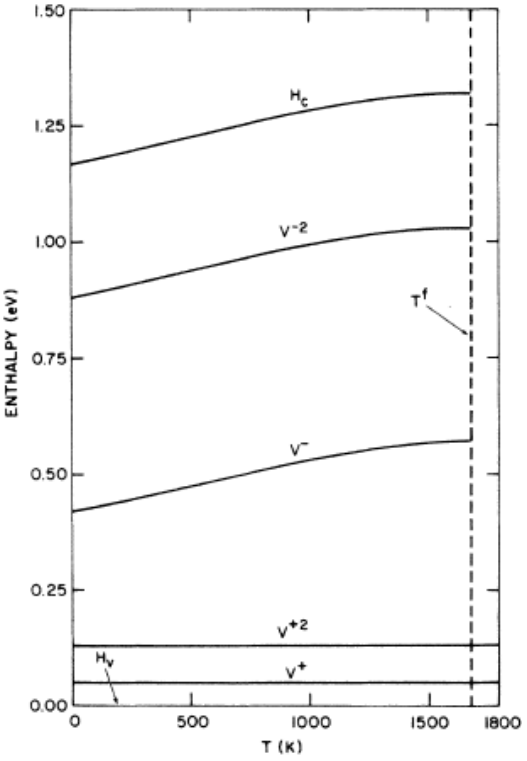

Fig. 2.2 Variation of the enthalpies of silicon vacancy ionization levels (and of the band gap) as a function of temperature. Reprinted figure with permission from Van Vechten, JA (1986) Phys Rev B: Condens Matter 33: 2677. Copyright (1986) by the American Physical Society.

2.2.2 Ionization Entropy

Formation entropies for defects can contain several contributions, including configurational degeneracy, lattice mode softening due to bond cleavage, and ionization (Van Vechten and Thurmond 1976b, a). Our principal concern here is the ionization contribution, which helps govern charge-mediated effects. There exists significant theoretical and experimental evidence to suggest that the ionization entropy $\Delta S^f_{X^q}$ can be very large for certain kinds of native defects such as vacancies. The main contribution to $\Delta S^f_{X^q}$ originates from electron-phonon coupling near the vacancy, leading to lattice-mode softening (Van Vechten and Thurmond 1976a; Dev and Seebauer 2003). The magnitude can be calculated by considering either the effect of thermal vibrations upon the electronic defect levels or the effect of the thermally excited electronic states upon the lattice vibration mode frequencies (Van Vechten 1980), although the latter method has proven more useful for simple estimates (Van Vechten and Thurmond 1976a).

In this perspective, the band gap energy E_g of a bulk semiconductor crystal corresponds to the standard chemical potential for creating a delocalized hole at the valence band maximum and a delocalized electron at the conduction band minimum.

Such creation might occur thermally or by photoexcitation. The magnitude of E_g can be obtained from the empirical Varshni relation given in Eq. 2.24.

Standard thermodynamic relations require that the entropy change E_g for formation of the electron-hole pair obeys (Thurmond 1975):

$$\Delta S_{cv}\left(T\right) = -\frac{\partial \Delta E_{cv}}{\partial T} = \frac{\alpha T\left(T+2\beta\right)}{\left(T+\beta\right)^2}. \tag{2.29}$$

Ionization of a defect represents another mechanism for creating two new carriers of opposite charge. One of the carriers roams the crystal in a delocalized way, while the other remains bound in the vicinity of the defect. The delocalized carrier contributes to ΔS_{cv} the way any delocalized carrier would. The effect of the bound carrier depends upon its degree of localization, however. If that carrier is loosely bound to the defect and therefore largely delocalized, the entropy for the ionization event clearly matches ΔS_{cv}.

If the carrier is tightly bound to the defect, however, and hovers close to it, the contribution to ΔS_{cv} is more difficult to estimate *a priori*. To make such an estimate, Van Vechten and Thurmond examined experimental data for the entropies of optical transitions in Si, Ge, GaAs and GaP between various points in the Brillouin zone. These data were derived from the temperature dependence of the various gaps as determined by optical reflectance. For Si the reported entropies suffered considerable uncertainties, but values remained within a factor or two of ΔS_{cv}. Since that compilation, more data have become available for Si that confirm the early results, including data for the E_2 and E_0' direct gaps up to 1,000 K (Jellison and Modine 1983) and for the E_2, E_0', E_1 and E_1' critical points up to 600 K (Lautenschlager *et al.* 1987). The optical results indicate that, at least for the four semiconductors examined, mode-softening effects from e^-–h^+ pair formation are insensitive to the final state charge distribution, so that, like the case of charges loosely bound to the defect,

$$\Delta S^f_{X^q}\left(T\right) \approx \Delta S_{cv}\left(T\right) \tag{2.30}$$

for single ionization events regardless of whether ionization results in a positive or negative vacancies (Van Vechten and Thurmond 1976a). Note that this argument should apply quite directly to the surface as well as the bulk, since the reflectance data on which the argument rests are sensitive primarily to surface optical susceptibilities. (Linear optical susceptibilities typically lie close to those of the bulk in any case.) Unlike the argument used for loosely bound carriers, however, Eq. 2.30 depends on data only for specific semiconductors – data that verify the conclusion only approximately.

These arguments suggest that $\Delta S_{cv}(T)$ can be used to estimate $\Delta S^f_{X^q}\left(T\right)$ regardless of the degree of localization of the bound charge. However, the reliability of the estimate does depend upon the degree of localization, which fortunately can be obtained with ease from DFT calculations.

A consequence of the correspondence between $\Delta S_{cv}(T)$ and $\Delta S^f_{X^q}\left(T\right)$ is that, as T increases and E_g decreases, free energies referenced to the valence band maximum

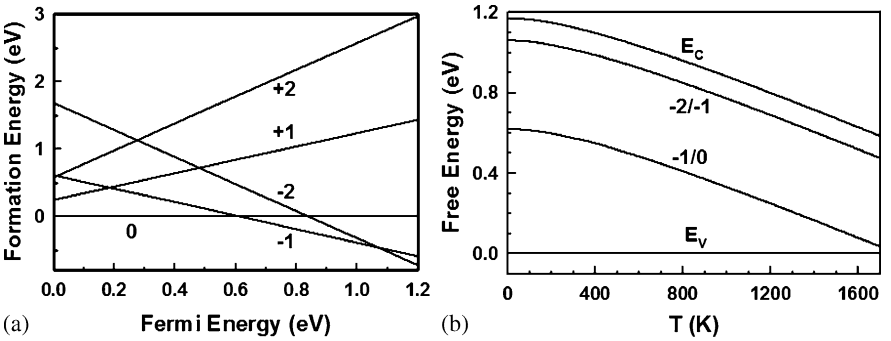

Fig. 2.3 (a) Formation energies of various dimer vacancy charge states on Si(100)–(2×1) as a function of Fermi energy at 0 K. The formation energy is referenced to the neutral dimer vacancy and the Fermi energy is referenced to the valence band maximum. The charge state with the lowest formation energy at a given Fermi energy has the highest concentration. (b) Variation of the dimer vacancy ionization levels with temperature.

for vacancy ionization levels remain at a constant energy below the conduction band for negatively charged vacancies and remain a constant energy above the valence band for positively charged (Van Vechten and Thurmond 1976a). This consequence makes the ionization levels quite easy to calculate from DFT results. An example for the divacancy on the Si(100) surface is shown in Fig. 2.3.

2.2.3 Energetics of Defect Clustering

It is important to remember that the enthalpy of formation need not refer simply to the enthalpy of formation of a point defect such as a vacancy or interstitial. An expression must also exist to describe the enthalpy of defect cluster formation. The term "cluster" encompasses a wide variety of defects including the divacancy, di-interstitial, vacancy-dopant pair, etc. Numerous methods and approximations for calculating the formation enthalpy of a defect pair exist in the literature; this section will summarize the primary approaches and discuss their validity.

Consider a pair formed from two identical charged defects X^q and X^q according to the fairly simple reaction

$$X^q + X^q \rightarrow (XX)^{2q}. \tag{2.31}$$

Associated with this reaction is an enthalpy of pair formation or "binding energy." For simplicity, the following discussion will distinguish between two components of the binding energy of $(XX)^{2q}$. The Coulombic interaction and the short-range "chemical" interaction between defects X^q and X^q sum to yield the binding energy of the pair:

$$\Delta H_b\left(XX^{2q}\right) = \Delta H_{b,Coulombic}\left(XX^{2q}\right) + \Phi_{X^qX^q}. \tag{2.32}$$

This treatment applies to both bulk and surface clusters. For example, Kudriavtsev *et al.* have calculated surface binding energies with a similar model that takes into account both covalent and ionic contributions (2005).

A first-order approximation of the binding energy ΔH_b of the pair is obtained from the Coulomb interaction energy of the two defects as estimated in the fully screened, point charge approximation. The fully screened, point charge approximation is a reasonable estimate of the binding energy as long as the eigenstates of the two defects reside within the band gap and are, therefore, localized electronic states (Dobson and Wager 1989). In reality, only a fraction α of the Coulombic energy contributes to ΔH_b according to

$$\Delta H_{b,Coulombic}\left(XX^{2q}\right) = \frac{q^2 e^2 \alpha}{4\pi\varepsilon_0 \varepsilon_r r}, \tag{2.33}$$

where q is the integral value of the charge on each defect (*i.e.,* (+1), (−1), etc.), e is the unit electronic charge, r is the equilibrium nearest neighbor separation distance, ε_0 is the permittivity of free space, and ε_r is the relative dielectric constant of the material in question. A negative value of binding energy indicates that defect clustering is energetically favorable. The fraction α corresponds to the amount of association energy it takes to push the defect ionization levels out of the band gap.

Notice that the Coulomb energy between the two charges must be modified to account for the consequent polarization of the surrounding ions in the lattice. For some defect complexes, this can be accounted for with the static dielectric constant of the semiconductor, ε_r, which is a measure of the polarizability of the lattice. In other instances, especially when defects are situated on adjacent lattice sites, the continuum quantity ε_r does not sufficiently account for the local effects of lattice polarization. In such cases, the Coulombic binding energy is typically lower than the experimentally determined binding energy.

There is one additional portion of the overall pair binding energy to be considered, the short-range "chemical" interaction between X^q and X^q, $\Phi_{X^qX^q}$. This component is especially important for semiconductors having primarily covalent bonding character, as the concept of a Coulombic potential necessitates that a point defect be treated as a fixed core (Fahey *et al.* 1989). When charges arise from bound carriers with wave functions that extend to neighboring sites, this approximation is clearly not applicable. The non-Coulombic interactions between the defects can be summed into the term $\Phi_{X^qX^q}$, for which several different estimates exist. For instance, Ball *et al.* cite the applicability of the Buckingham potential model to defect modeling in CeO_2 and other oxide semiconductors (2005). According to this model

$$\Phi\left(r_{X^qX^q}\right) = A_{X^qX^q} \exp\left(-\frac{r_{X^qX^q}}{\rho_{X^qX^q}}\right) - \frac{C_{X^qX^q}}{r_{X^qX^q}^6}, \tag{2.34}$$

where $r_{X^qX^q}$ is the nearest neighbor distance between X^q and X^q, and $A_{X^qX^q}$, $\rho_{X^qX^q}$, and $C_{X^qX^q}$ are adjustable parameters. The parameters were selected to reproduce

the unit cell volumes of various relates oxides. Also, the pair interaction in a covalent material as a function of radial separation can be expressed as

$$\Phi(r) = \Phi_0 \exp\left[-\beta\left(r / r_{X^q X^q} - 1\right)\right], \tag{2.35}$$

where $r_{X^q X^q}$ is the nearest neighbor distance between X^q and X^q, and β and Φ_o are adjustable parameters (Cai 1999). β and Φ_0 can be determined by fitting experimental data consisting of elastic constants, lattice constants, and cohesive energy.

2.2.4 Effects of Gas Pressure on Defect Concentration

In many compound semiconductors, one of the constituent elements typically exists in gaseous form under laboratory or processing conditions. For example, the oxygen in metal oxides exists as O_2 gas. Upon heating in an environment having a low partial pressure of oxygen, some of the lattice oxygen escapes from the crystal structure and diffuses through the material into the gas phase, leaving behind oxygen vacancies and (depending upon reactions among defects) other kinds of defects as well. A reverse process can also take place if the ambient partial pressure of oxygen is high enough; oxygen can diffuse into the material and annihilate oxygen vacancies. Analogous phenomena occur in other compound semiconductors such as GaAs; at sufficiently high temperatures, both Ga and As have significant vapor pressures and can exchange with the corresponding vacancies within the GaAs crystal structure. Since As is the more volatile species, GaAs tends to lose As more readily when heated in vacuum.

Point defect concentrations in such cases depend upon ambient conditions (Kroger and Vink 1958; Sasaki and Maier 1999b, a), and can be calculated from equations derived via mass-action principles applied to all the relevant defects and charge carriers (Jarzebski 1973; Sasaki and Maier 1999b).

This approach has been applied quite extensively in the case of metal oxides. The equilibrium between a crystal MO and the gas phase is described according to

$$MO \equiv M_M^0 + O_O^0 \leftrightarrow MO^{(g)} \tag{2.36}$$

$$M_M^0 + O_O^0 \leftrightarrow M^{(g)} + \frac{1}{2} O_2^{(g)}. \tag{2.37}$$

At a fixed temperature, the concentration of defects in the bulk can be varied by altering the partial pressure of the ambient. When a neutral oxygen atom is added to the MO crystal lattice a new pair of lattice sites is created; the cation site remains vacant, creating a metal vacancy:

$$\frac{1}{2} O_2^{(g)} \leftrightarrow O_O^0 + V_M^0. \tag{2.38}$$

If the metal vacancy were to subsequently ionize to V_M^{-1}, the concentration of V_M^{-1} could be described as a function of oxygen partial pressure according to

$$\left[V_M^{-1}\right] = \frac{K_1 P_{O_2}^{1/2}}{p\left[O_O\right]}, \tag{2.39}$$

where K_1 is the equilibrium constant for Eq. 2.39 and p is the concentration of free hole carriers. Equations of this form can be written for other charge states as well. In the case of the vacancy in the (−2) state, the term p^2 would appear in the denominator, whereas for the neutral state p would not appear at all.

Oxides can also exchange metal atoms with the gas phase, although most experimental configurations do not allow independent control of metal gas phase pressure. However, metal vapor pressures are typically low, so that experiments that allow independent control of metal partial pressures still give good approximations to equilibrium conditions. When P_M is high, metal atoms fill metal vacancies in the bulk and create vacancies in the oxygen sublattice:

$$M^{(g)} \leftrightarrow M_M^0 + V_O^0. \tag{2.40}$$

Once oxygen vacancies ionize into the (+1) charge state, their concentration is given by

$$\left[V_O^{+1}\right] = \frac{K_2 P_M}{n\left[M_M^0\right]}. \tag{2.41}$$

Additionally, it should be noted that the electroneutrality condition must always be obeyed. This condition accounts for the fact that the overall crystal has no electrical charge, even though charged defects exist in the bulk:

$$n + \left[V_M^{-1}\right] = p + \left[V_O^{+1}\right]. \tag{2.42}$$

One final equilibrium expression,

$$n * p = K_i \tag{2.43}$$

arises from the equilibration of electrons and holes in the crystal. The ionized defects in MO are now described by a series of algebraic equations containing seven variables: n, p, $\left[V_M^{-1}\right]$, $\left[V_O^{+1}\right]$, P_M, P_{O_2}, and T, where T is the absolute temperature of the system. Normally T and P_{O_2} are taken as independent variables; P_M is then a dependent variable. This treatment can be generalized to materials with a larger variety of charged defects and electrical states.

In this treatment, the charge state dependence arises from the equilibrium constants; no separate contributions to the free energy, entropy, or enthalpy of ionization are broken out. This approach differs decidedly from that of Van Vechten, who explicitly references concentrations of charged species to the corresponding concentrations of neutral species.

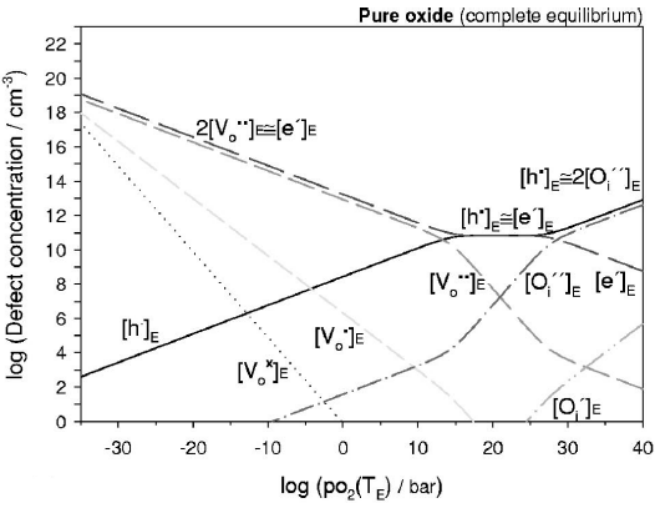

Fig. 2.4 Brouwer diagram of a pure oxide in complete equilibrium at 800ºC from (Sasaki and Maier 1999), where the concentrations of charged and neutral oxygen vacancies and interstitials are shown as a function of oxygen partial pressure. Reprinted with permission from Sasaki K, Maier J (1999) J Appl Phys 86: 5427. Copyright (1999), American Institute of Physics.

Based on equations such as 2.36 through 2.43, a plot of species concentrations vs. oxygen partial pressures can be subdivided into regions in which various defects predominate. To make this subdivision, it is necessary to know (either exactly or approximately) the values of all of the equilibrium constants at a given temperature. This complicated system of equations is often visualized by applying the graphical method proposed by Brouwer (1954). It is thus common to find the concentration of charged defects in TiO_2, ZnO, UO_2, and CoO plotted as a function of oxygen partial pressure as illustrated in (Fig. 2.4), where either the valence band maximum or conduction band minimum is used as the reference for the Fermi energy. In this instance, the temperature is held constant at 800ºC. The change in the diagram as a function of temperature will be related to the enthalpies of the various defect formation reactions.

2.3 Thermal Diffusion

Bulk diffusion in semiconductors is typically mediated by point defects such as vacancies and interstitials, which may exchange with the lattice and with defect clusters (which sometimes play a role as reservoirs of defects) (Pichler 2004; Chang *et al.* 1996; Fu-Hsing 1999; Seeger and Chik 1968; Hu 1973; Casey *et al.* 1973). The situation is similar for surface diffusion, although the relevant defects are typically surface vacancies and adatoms, which can exchange with surface lattice sites and islands.

For both the bulk and the surface, an atomistic description of the diffusion rate exists for native point defects, based on the work of Einstein and Smoluchowski. That description quantifies the defect motion (before exchange with the lattice or other reservoirs) in terms of a diffusion coefficient D. In a single dimension (say, x), component D_x of the diffusion coefficient in that direction is defined in terms of the mean square x-displacement $\overline{\Delta x^2}$ of the diffusing species and the time interval t during which diffusion takes place, according to

$$D_x = \frac{\overline{\Delta x^2}}{2t}. \tag{2.44}$$

In the case of diffusion in N dimensions (2 for surface, 3 for bulk) with mean square displacement $\overline{\Delta r^2}$, this equation generalizes to

$$D = \frac{\overline{\Delta r^2}}{2Nt}. \tag{2.45}$$

Treatments of diffusion in this context often examine random hopping motion between well-defined, energetically favorable sites (Pichler 2004). If Γ represents the hopping frequency between sites and L is the hop length between them, then the diffusion coefficient can be recast as:

$$D = \frac{\Gamma L^2}{2N}. \tag{2.46}$$

Since thermal diffusion of defects on or within semiconductors generally involves some form of bond stretching or breakage, the hopping frequency typically incorporates a temperature dependence in Arrhenius form. Zener (1951), Vineyard (1957), Rice (1958), and Flynn (1968) have all presented theories for the jump frequency of a diffusing defect in the bulk, where Γ can be expressed as (for temperatures above the Debye temperature):

$$\Gamma = \Gamma_0 \cdot \exp\left(\frac{\Delta S_m}{k}\right) \cdot \exp\left(-\frac{\Delta H_m}{kT}\right) \tag{2.47}$$

where Γ_0 stands for a weighted mean frequency, often called an "attempt frequency," and ΔS_m and ΔH_m respectively represent the entropy and enthalpy of migration, T is the absolute temperature, and k is Boltzmann's constant. Related descriptions exist for surface diffusion (Gomer 1996).

D is sometimes written in simpler Arrhenius form

$$D(T) = D_0 \exp\left(-E_a / kT\right) \tag{2.48}$$

where E_a is the activation energy for diffusion, D_0 is the pre-exponential factor. Clearly $E_a = \Delta H_m$ in this treatment. Comparing Eqs. 2.47 and 2.48 indicates that

$$D_0 = \frac{\Gamma_0 \exp(\Delta S_m / k) L^2}{2n}. \tag{2.49}$$

For both bulk and surface intrinsic diffusion, Γ_0 usually lies near a vibrational frequency (about the Debye frequency) of 10^{12} s^{-1}, while L is typically an atomic bonding distance near 0.3 nm. Thus, in the absence of significant entropy effects during diffusion, the pre-exponential factor lies near 10^{-3} cm^2/s both in the bulk and on the surface. Significant deviations from this value are often observed, however, particularly for surface diffusion (Seebauer and Jung 2001).

An individual type of defect can sometimes diffuse by more than one pathway. Self-diffusion of the silicon interstitial is a primary example, where numerous possible pathways have been identified (Lee *et al.* 1998b; Kato 1993; Munro and Wales 1999; Sahli and Fichtner 2005). For the case of oxide semiconductors, where significant deviations from stoichiometry often occur, the dominant diffusion mechanism may depend on the partial pressure of the ambient (Bak *et al.* 2003; Diebold 2003; Hoshino *et al.* 1985; Jun-Liang *et al.* 2006; Kohan *et al.* 2000; Millot and Picard 1988; Oba *et al.* 2001; Tomlins *et al.* 1998; Erhart and Albe 2006).

Defects of different types can sometimes bind together (while retaining their individual identities) to diffuse as a pair. For example, vacancies can be attracted to substitutional impurities by various long and short range electrostatic and strain forces, leading to binding energies on the order of 1 eV or more (Nelson *et al.* 1998). The exchange of places between the impurity and the vacancy induce diffusional motion of both species (Belova and Murch 1999). As another example, interstitials can bind to intrinsic or extrinsic defects and migrate via a "pair diffusion" mechanism, frequently also called an "interstitialcy" mechanism (although the former will be used throughout the remainder of this text). The impurity atom exchanges with the lattice on every hop, instead of squeezing between lattice sites for multiple hops before exchanging. The impurity atom does not necessarily carry the same host atom with it; over time, the impurity atom can exchange with any number of different host atoms.

The atomistic perspective outlined above constitutes the basis of most theoretical methods for estimating diffusion coefficients, as well as interpretation of experimental methods that directly image atomic motion. On length scales longer than a few atomic diameters, however, the total rate of mass transport within the bulk or on the surface depends not only upon the mobility of defects, which the equations given above describe, but also upon the number of those defects available to move. This total rate is the focus of primary concern in many practical applications, such as the diffusion of dopants within microelectronic devices and heterogeneous catalysis, sintering, and corrosion on surfaces. In principle, several types of defects can contribute to the overall motion. Such behavior has been reported for bulk silicon, where certain measurements have been interpreted in terms of separate diffusional pathways involving vacancies and interstitial atoms (Ural *et al.* 1999, 2000; Bracht and Haller 2000). However, more typically a single defect type dominates the transport. For example, bulk diffusion can be mediated by the directional migration of vacancies or interstitials, the displacement of lattice atoms into interstitial sites, or the interchange of diffusing atoms between substitutional and interstitial sites in the crystal lattice (Sharma 1990). The latter mechanism is often referred to as "kick-out" diffusion.

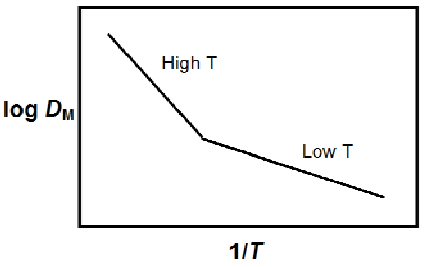

Fig. 2.5 Sketch of an Arrhenius plot for mesoscale surface mass transport on metals, showing two temperature regimes.

Similar principles apply to surface diffusion. Migration on semiconductor substrates has not been studied to the extent of that in the bulk. In analogy to bulk diffusion, however, different migration mechanisms dominate on the surface as a function of temperature, Fermi energy, and stoichiometry. For metals, a large body of aggregated experimental data for nickel, tungsten, silicon, germanium, aluminum oxide, and other materials indicates that two distinct temperature regimes of Arrhenius behavior exist for surface self-diffusion (Doi *et al.* 1995; Bonzel 1973; Seebauer and Jung 2001; Seebauer and Allen 1995; Mills *et al.* 1969; Plummer and Rhodin 1968; Binh and Melinon 1985; Tsoga and Nikolopoulos 1994; Fukutani 1993), as sketched schematically in Fig. 2.5. The trends appear to arise from adatom-dominated transport at low temperatures and vacancy-dominated transport at high temperatures. It is reasonable to suppose that similar mechanisms operate on semiconductor surfaces, although insufficient experimental data currently exist to verify that idea.

A continuum approach often proves more useful for quantifying diffusion in many kinds of experimental measurements taken at length scales longer than a few atoms (Seeger and Chik 1968). When a spatially inhomogeneous distribution of defects exists in the bulk or on the surface, the species migrate to reestablish equilibrium. In the continuum description, a diffusion coefficient D can be defined assuming that the chemical potential of the diffusing species X scales linearly with its concentration [X]. (Note that other factors sometimes influence the chemical potential gradient, such as strong curvature in surface scratch decay experiments.) In the absence of electric fields, the flux J of the diffusing species obeys Fick's 1st law:

$$J = -D\nabla[X]. \tag{2.50}$$

The dependence of [X] on time and space is described by Fick's 2nd law

$$\frac{\partial[X]}{\partial t} = \nabla \bullet \left(D\nabla[X]\right). \tag{2.51}$$

Note that "species" must be defined carefully. For example, for purposes of Fick's laws, an interstitial dopant atom constitutes a different species than a substitutional one. Failure to make this distinction sometimes leads to erroneous discussion of "non-Fickian diffusion" when kick-in/kick-out reactions interconvert the interstitial and substitutional species. Diffusion profiles measured at short times (before the mobile species has exchanged a significant number of times

with the lattice) yield non-Fickian shapes such as exponentials (Vaidyanathan *et al.* 2006b).

In surface diffusion, these considerations apply as follows. The literature often defines a mesoscale diffusivity D_M (Seebauer and Jung 2001; Bonzel 1973) (called the "mass transfer diffusivity" in older literature) that incorporates both the hopping diffusivity D_I (called "intrinsic diffusivity" in older literature) of a defect and the concentration of mobile defects [X_{mobile}], normalized by the concentration of substrate atoms [substrate] (not to be confused with [S], the concentration of available lattice sites in the crystal:

$$D_M = D_I \frac{[X_{mobile}]}{[substrate]}. \tag{2.52}$$

Experimental techniques that are at least indirectly sensitive to the creation and migration of mobile defects generally measure D_M rather than D_I. Example techniques (Seebauer and Jung 2001) include scratch decay and low-energy electron microscopy, wherein mobile atoms are typically formed from step, kink, or terrace sites. D_I is commonly measured by methods that can track individual atoms, such as scanning tunneling microscopy (STM) and field ion microscopy (FIM). D_M typically has a stronger temperature dependence than D_I due to the added temperature dependence of C_{eq}, which varies due to the creation and exchange of adatoms or vacancies with the bulk (Kyuno *et al.* 1999) or other surface features such as steps (Ehrlich and Hudda 1966; Breeman and Boerma 1992), islands (Beke and Kaganovskii 1995), and extrinsic defects (Heidberg *et al.* 1992; Hansen *et al.* 1996).

The kink sites at steps or island edges can mediate both adatom and vacancy diffusion mechanisms that operate in parallel. Without being destroyed themselves, kinks can independently create both adatoms and terrace vacancies (Blakely 1973). Although adatoms and vacancies can form and annihilate as pairs on terraces, equilibrium between these species does not require their coverages to be equal. Moreover, one species can dominate mass transport through superior numbers even if its mobility falls below that of the other species.

The definition of D_M given in Eq. 2.52 contains two temperature-dependent factors for the mobile species: the hopping diffusivity

$$D_I = D_{0I} \exp(-E_I / kT), \tag{2.53}$$

and the equilibrium concentration

$$C_{eq} = C_{sub} \exp(-\Delta G_f / kT). \tag{2.54}$$

Substitution into Eq. 2.52 for D_I and C_{eq} and decomposition of ΔG_f into its constituent enthalpy ΔH_f and entropy ΔS_f yields:

$$D_M = D_{0I} \exp\left(\frac{\Delta S_f}{k}\right) \exp\left(\frac{-(\Delta H_f + E_I)}{kT}\right). \tag{2.55}$$

For mesoscale diffusion, an effective pre-exponential factor can be defined together with a corresponding activation energy

$$D_{0M} = D_{0I} \exp(\Delta S_f / k) \tag{2.56}$$

$$E_M = \Delta H_f + E_I . \tag{2.57}$$

The form of Eq. 2.57 shows that a diffusion mechanism with high E_M can dominate a mechanism with low E_M if the former has a much higher value of D_{0M} and if the temperature is sufficiently high. Such diffusion mechanisms working in parallel can produce the temperature dependence shown in Fig. 2.5.

Regardless of the specific bulk or surface diffusion mechanism, the charge state of the primary diffusing defect can affect its rate of hopping. For example, changing the charge state of a bulk interstitial atom affects not only its effective size (and therefore its ability to squeeze between lattice atoms) but also its ability to chemically bond to the surrounding atoms. In silicon, for example, the energy barrier for the migration of V^{+2} differs from that of V^{-2} (Bernstein *et al.* 2000; Kumeda *et al.* 2001; Watkins 1967, 1975, 1986; Watkins *et al.* 1979). Such effects can, in principle, show up in the pre-exponential factor as well as the activation energy.

Thus, there are two ways for charge state to affect the rate of motion of a defect over length scales greater than atomic: changes in concentration and changes in hopping rate. When multiple charge states for a defect exist simultaneously, their effects are typically additive. For example, an effective diffusivity of self-interstitials can be expressed as

$$D_i^{eff} = D_{i^0}\left(\frac{\left[X_i^0\right]}{\left[X_i\right]}\right) + D_{i^{+1}}\left(\frac{\left[X_i^{+1}\right]}{\left[X_i\right]}\right) + D_{i^{-1}}\left(\frac{\left[X_i^{-1}\right]}{\left[X_i\right]}\right) + \ldots \tag{2.58}$$

where $[X_i]$ is the total concentration of interstitials (in all charge states). The relative importance of each of these terms depends upon the position of the Fermi energy.

2.4 Drift in Electric Fields

Semiconductor *pn* junctions and heterojunctions are the foundation of most major microelectronic devices, and these structures contain appreciable built-in electric fields. Such fields act on mobile charged defects (Sheinkman *et al.* 1998) during processing and subsequent device use. These fields, as well as their interactions with electrically active defects introduced during the fabrication process, can dramatically degrade device performance (El-Hdiy *et al.* 1993). The reduction in size scale of these devices has caused the magnitudes of these electric fields to progressively rise.

When an electric field ε of 10^4 to 10^6 V/cm is applied along with thermal diffusion from a constant source, field-aided diffusion takes place (Sharma 1990) according to:

$$J = -D\frac{\partial[X]}{\partial x} + q\mu[X]\varepsilon(x) \tag{2.59}$$

where [X] is the concentration of defect X and q is the charge of defect X. The mobility μ can be approximated roughly as qD/kT. The transport rate of charged defects can be either retarded or enhanced depending on the direction of the field. For a complete solution of the equations of motion for the defects, this transport equation must be solved together with Poisson's equation for the electrostatic potential Ψ:

$$\nabla^2\Psi = \frac{e}{\varepsilon}\left(n - p + \sum_i q_i\left[X_i^q\right]\right) \tag{2.60}$$

where n and p are the number of electrons and holes in the conduction and valence bands, respectively, q_i is the charge associated with the defect X_i with concentration $[X_i]$, and e is the electronic charge. For example, q_i would take on a nominal charge of (+1) for singly ionized acceptors and (−1) for singly ionized donors.

Field-assisted diffusion also occurs on semiconductor surfaces (Yagi *et al.* 1993; Kawai and Watanabe 1997). Such behavior has been observed most notably in the imaging of charged defects with scanning tunneling microscopy. Tip-induced electric fields affect the electronic structure of a semiconductor surface containing native defects (Ness *et al.* 1997b, a; Saranin *et al.* 1997).

2.5 Defect Kinetics

The rate expressions that govern the generation, destruction and clustering of point defects are important for predicting and interpreting transient behavior that commonly occurs during semiconductor processing as well as certain experimental techniques designed to detect defects. The following sections outline some basic principles of defect reaction kinetics, as well as the kinetics of defect charging.

2.5.1 Reactions

Although rate expressions for defect reactions can be developed in the abstract, it is perhaps more instructive to set such a presentation in the context of a specific case to bring out the nuances of kinetic integration that typically characterize a reaction network of defects within a typical semiconductor. The focus here will be on defects within the bulk, but analogous descriptions apply to surfaces.

The specific example we will use is boron acting as a p-type dopant within silicon (Jung *et al.* 2004b). Microelectronic devices comprise an obvious application. When boron is the primary impurity, it resides primarily in substitutional sites in a (–1) charge state. However, the substitutional boron can interact with interstitial silicon through a kick-out mechanism and become interstitial itself. In typical p-type material, interstitial boron exists as B_i^{+1}, interstitial silicon as Si_i^{+2}. Quantum calculations have also pointed to the existence of a well-defined complex of substitutional boron and the silicon interstitial:$(B_{Si}Si_i)^{+1}$. Boron can diffuse (and participate in reactions such as clustering) either as the free interstitial or through pair diffusion via $(B_{Si}Si_i)^{+1}$. Similar expositions detail the kinetics of defect formation and annihilation in GaN (Tuomisto 2005), ZnO (Kotlyarevsky *et al.* 2005), and Si (Pichler 2004).

Figure 2.6 details the interaction among the various boron and silicon species. Breakup of the $(B_{Si}Si_i)^{+1}$ complex to yield interstitial species occurs by two pathways that are each kinetically first-order in the concentration of $(B_{Si}Si_i)^{+1}$. Dissociation to yield free Si_i^{+2} is denoted by the rate r_{dis}, while dissociation via kick-out to yield free B_i^{+1} is denoted by r_{ko}. The reverse reaction of kick-in is also fundamentally first-order, depending only on the concentration $[B_i^+]$ because each B_i is completely surrounded by lattice Si atoms with which it can react. The association reaction between Si_i^{+2} and B_{Si}^{-1} is second-order, however, because B_{Si}^{-1} is by far the minority species in terms of lattice site occupation. Although an activation barrier may exist in principle when these species get close enough to react, the opposite charges on the reactants and the negative free energy of formation for the complex give reasons to believe that the complex forms with no barrier. A rate expression describing standard diffusion limitation by reactants (Laidler 1980) therefore is warranted.

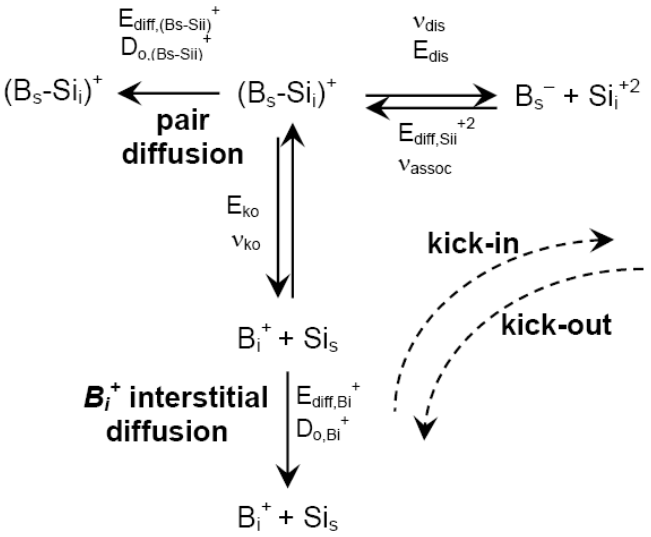

Fig. 2.6 Composite reaction network for reactions of boron defects in silicon, incorporating the kick-out and pair diffusion mechanisms.

The reaction stoichiometries are:

$$\left(B_{Si}Si_i\right)^{+1} \rightarrow B_i^{+1} + Si_{Si} \quad \text{(kick-out)} \tag{2.61}$$

$$B_i^{+1} + Si_{Si} \rightarrow \left(B_{Si}Si_i\right)^{+1} \quad \text{(kick-in)} \tag{2.62}$$

$$\left(B_{Si}Si_i\right)^{+1} \rightarrow B_{Si}^{-1} + Si_i^{+2} \quad \text{(dissociation)} \tag{2.63}$$

$$B_{Si}^{-1} + Si_i^{+2} \rightarrow \left(B_{Si}Si_i\right)^{+1} \quad \text{(association).} \tag{2.64}$$

The corresponding rate expressions are:

$$r_{ko} = k_{ko} \exp\left(-E_{ko} / kT\right)\left[\left(B_{Si}Si_i\right)^{+1}\right] \tag{2.65}$$

$$r_{ki} = k_{ki} \exp\left(-E_{ki} / kT\right)\left[B_i^{+1}\right] \tag{2.66}$$

$$r_{dis} = k_{dis} \exp\left(-E_{dis} / kT\right)\left[\left(B_{Si}Si_i\right)^{+1}\right]. \tag{2.67}$$

$$r_{assoc} = k_{assoc}\left[B_{Si}^{-1}\right]\left[Si_i^{+2}\right] \tag{2.68}$$

with

$$k_{assoc} = 4\pi a D_{assoc} \tag{2.69}$$

where $D_{assoc} = D_{B_{Si}^{-1}} + D_{Si_i^{+2}}$, with $D_{B_{Si}^{-1}} << D_{Si_i^{+2}}$. Here, a represents a reaction distance or "capture radius."

From these expressions, along with maximum likelihood estimates for the corresponding activation energies and pre-exponential factors, it is possible to determine the conditions under which the interstitial diffusion mechanism dominates pair diffusion (Jung *et al.* 2004b).

The kinetic treatment of point defects and defect pairs in boron-implanted Si can be extended to describe the further associations of interstitials into clusters of indefinitely large sizes during postimplant annealing (Jung *et al.* 2004a). The association reaction between Si_i or B_i and a cluster is second-order. A rate expression describing standard diffusion limitation is appropriate:

$$r_{assoc} = k_{assoc}[cluster][B_i \text{ or } Si_i] \tag{2.70}$$

with

$$r_{assoc} = 4\pi a D_{B_i} \text{ or } r_{assoc} = 4\pi a D_{Si_i} \tag{2.71}$$

where clusters have been assumed to be much less mobile than free interstitials.

Dissociation kinetics is more problematic, since the rate expressions used in the literature sometimes have inadequacies. The rate expression commonly employed in literature for dissociation kinetics assumes the following form (Stolk *et al.* 1997):

$$r_{dis} = \frac{D_{\text{int}}}{a^2} \exp(-E_b / kT)[cluster] \tag{2.72}$$

where E_b denotes the binding energy and D_{int} the interstitial diffusivity. Eq. 2.72 is problematic in several ways, but its greatest flaw originates from its assumption that dissociation involves two sequential steps: interstitial release from the cluster followed a diffusional hop away from the cluster. However, except for $(B_{Si}Si_i)^{+1}$, the barrier to interstitial release (for which the binding energy sets only a lower bound) is significantly larger than that for diffusional hopping. Since the pre-exponential factor is likely to be the same for both release and hopping (*i.e.,* close to a Debye frequency), interstitial release must be rate limiting in this reaction sequence. It can be easily shown that in a reaction sequence including a rate-limiting step, steps after the rate limiting one exert no influence whatever on the overall rate. Thus, rate expressions that include parameters from steps following the rate limiting one must in principle be incorrect. In general, simple models for elementary dissociation reactions employ first-order kinetics and cast rate constants as the mathematical product of an attempt frequency and an exponential Boltzmann factor containing a transition-state activation barrier (which may not be the same as the binding energy). Regarding the pre-exponential factor, the Debye frequency for the host material represents a good first approximation.

Since in this particular case, cluster dissociation energies generally increase with cluster size, a general model for interactions among defects and clusters can telescope the entire cluster dissociation cascade (from large to small clusters) into a computationally manageable set of events There are many cluster dissociation pathways due to the varying stoichiometries of larger clusters. Consequently, a nearly continuous distribution of dissociation energies is well suited to approximating the activation energies of the pathways. For practical applications, such a model has proven capable of providing insight into how the initial conditions and subsequent heating steps in rapid thermal annealing affect transient enhanced diffusion (Gunawan *et al.* 2003). These can be tailored to minimize the size and number of defect clusters that diffuse within the bulk.

Use of such a model can be accomplished within the context of a differential equation solver that produces numerical results for the coupled equations just outlined. However, some engineering applications employ unsteady-state heating protocols such as linear ramps. Numerical simulations can certain handle such situations, but sometimes an analytical or nearly-analytical approach is more useful for quick estimates of defect behavior. For example, annealing to remove ion implantation damage in *pn* junction formation is limited in part by transient enhanced diffusion (TED) of dopants, often leading to unacceptable spreading of the original dopant profile (Jung *et al.* 2003). Annealing usually employs a linear ramping program that raises the solid temperature over 1,000°C within about 1 s.

Although the system is transiently heated, some straightforward approximations permit important insights to be gained into defect behavior and the resulting dopant diffusion. Under common heating conditions, it can be shown that the diffusion of boron in TED is mediated by the motion of free B_i (Jung *et al.* 2004b). The motion of free B_i is hampered by boron exchange with lattice sites. When this exchange mechanism dominates, boron moves while it is a free interstitial, but is rapidly immobilized when $(B_{Si}Si_i)$ releases Si_i. The trapped boron can move again

only after lengthy period of waiting for association with another free Si interstitial. The time constant describing this waiting period is $(k_{assoc}[\mathrm{Si_i}])^{-1}$, where k_{assoc} denotes the rate constant for the association reaction between B_{Si} and Si_i. By defining t_{max} as a characteristic time over which the wafer remains near the peak temperature, the number of liberation events can be estimated from the ratio of t_{max} to the characteristic time $(k_{assoc}[\mathrm{Si_i}])^{-1}$ for the association reaction. Then the degree of profile spreading can be estimated from Gunawan *et al.* as

$$x^2 = \frac{6D_{diff,B_i}}{k_{ki}} k_{assoc}\left[Si_i\right] t_{\max}\left(\frac{1-b}{b}\right) \tag{2.73}$$

where k_{ki} and D_{diff,B_i} represent respectively the rate constant for kick-in and the diffusion coefficient for B_i hopping. The branching ratio b describing the pathways for the dissociation reaction of $B_{Si}Si_i$ to form B_i and Si_i is given by

$$b = \frac{r_{B_{Si}Si_i \to B_{Si}+Si_i}}{r_{B_{Si}Si_i \to B_{Si}+Si_i} + r_{B_{Si}Si_i \to B_i+Si}}. \tag{2.74}$$

Several easily satisfied assumptions are required for these equations to hold. First, dissociation must occur in the equivalent of a single step. Second, interstitial reassociation with the most actively dissociating clusters must be neglected. Lastly, the distribution of cluster dissociation energies must be wider than $1.5kT$. Under these circumstances, a closed-form analytical expression can be obtained connecting each temperature in the linear ramp with the dissociation energy E^* of the most active dissociating species. Simulations can then be used to understand why heating rate affects cluster dissociation energy and thus cluster concentration.

2.5.2 Charging

Defects exchange charge with the conduction and valence bands via either thermal or radiative processes. In the thermal processes, the defect captures or emits a charge carrier directly, with a rate that is generally quite fast for defect eigenstates close to the bands, but sometimes much slower (many seconds) for levels lying deep within the band gap. A detailed discussion of such kinetics can be found in Landsberg's book (Landsberg 1991).

Radiative processes involve the absorption or emission of a photon. When the semiconductor is illuminated, the rate of electron-hole pair generation g_E obeys two continuity (mass balance) equations:

$$g_E - \frac{d\Delta n}{dt} = \frac{\Delta n}{\tau_n} = \frac{1}{\tau_{n0}}\left[\frac{\left(n_0 + n_1 + \Delta n\right)\left(\Delta n - \Delta p\right)}{N} + \frac{\Delta n n_1}{n_0 + n_1}\right] \tag{2.75}$$

$$g_E - \frac{d\Delta p}{dt} = \frac{\Delta p}{\tau_p} = \frac{1}{\tau_{p0}}\left[\frac{\left(p_0 + p_1 + \Delta p\right)\left(\Delta p - \Delta n\right)}{N} + \frac{\Delta p p_1}{p_0 + p_1}\right], \tag{2.76}$$

where n_0 and p_0 are the electron and hole concentrations in thermal equilibrium, τ_n and τ_p are the electron and hole lifetimes, and N is the recombination center density (Schmidt *et al.* 1998). The time constants τ_{n0} and τ_{p0} for capture of electrons and holes by defects (inducing a change in ionization state), depend upon the capture cross sections σ_n and σ_p of the defect, and also upon the defect concentration and the thermal velocities of electrons and holes υ_{th} equal to $\sqrt{3kT/m^*}$. The times constants are given by:

$$\tau_{n0} = \frac{1}{N\sigma_n \nu_{th}} \tag{2.77}$$

$$\tau_{p0} = \frac{1}{N\sigma_p \nu_{th}}. \tag{2.78}$$

The statistical factors n_1 and p_1 are the equilibrium concentrations of electrons and holes, respectively, when the Fermi level coincides with the eigenstate of the defect E_T:

$$n_1 = N_C \exp\left(\frac{E_T - E_c}{kT}\right) \tag{2.79}$$

$$p_1 = N_V \exp\left(\frac{E_c - E_g - E_T}{kT}\right), \tag{2.80}$$

where E_c is the conduction band edge energy and E_g the band gap.

Under steady-state conditions, the time-dependent terms in these equations vanish, and various general analytic solutions exist (Shockley and Read 1952). Shockley and Read presented one such solution, with the underlying assumption of spin nondegeneracy. Additional simplifications lead to the Shockley–Read–Hall (SRH) model commonly used today (Macdonald and Cuevas 2003), and involve eliminating N, rearranging, and using the identities $n_0/(n_0+n_1)=p_0/(p_0+p_1)$ and $p_1n_1=p_0n_0$ to obtain:

$$g_E = \frac{\Delta n}{\tau_n} = \frac{\Delta p}{\tau_p} = \frac{p_0\Delta n + n_0\Delta p + \Delta n\Delta p}{\tau_{p0}\left(n_0 + n_1 + \Delta n\right) + \tau_{n0}\left(p_0 + p_1 + \Delta p\right)}. \tag{2.81}$$

Further manipulation of this equation, along with the assumption of negligible excess carrier densities, leads to the following expression for the charge carrier lifetime:

$$\tau_{SRH} = \tau_n = \tau_p = \frac{\tau_{p0}\left(n_0 + n_1 + \Delta n\right) + \tau_{n0}\left(p_0 + p_1 + \Delta p\right)}{n_0 + p_0 + \Delta n}. \tag{2.82}$$

The concept of a "demarcation level" is also sometimes used to describe exchange of charge with the valence and conduction bands. Whereas the ionization level relates to thermodynamic equilibria, the demarcation level focuses on kinetic rates of charge capture. The hole demarcation level is defined as the ionization

level at which the rate of hole emission equals the rate of electron capture. That is, a hole at a level equal to the hole demarcation level has an equal probability of being thermally excited to the valence band as it does recombining with a electron in the conduction band. Depending on the position of a defect ionization level relative to the demarcation level, one process or the other will be more likely to occur. The location of the hole demarcation level is extracted from the following definition

$$E_F - E_{Dp} = kT \ln\left[\frac{n}{p}\left(\frac{\sigma_n v_n}{\sigma_p v_p}\right)\right] \tag{2.83}$$

where σ are the capture cross sections and v thermal velocities of electrons (n) and holes (p), n and p the concentrations of electrons and holes, and E_{Dp} the hole demarcation level (Bube 1992). If a measurable phenomena occurs that changes a particular set of defect levels from recombination centers to hole traps, a measurement of electron density allows for the determination of the demarcation level.

A corresponding expression can be derived from the electron demarcation level.

2.6 Direct Surface-Bulk Coupling

Researchers have expended substantial effort comparing the physics of bulk solids with those of free surfaces and solid interfaces. Curiously, much less attention has focused upon the direct coupling between these phenomena. Only a handful of papers have considered topics such as bulk quenching of surface exciton emission (David *et al.* 1989), bulk-influenced surface state behavior at steps on metals (Baumberger *et al.* 2000), and bulk doping effects on surface band bending in semiconductors (Vitomirov *et al.* 1989; Kuball *et al.* 1994; King *et al.* 2007). While Vitomirov *et al.* considered the effects of the semiconductor bulk on surface electronic properties; other work has shown that surface and interface electronic properties affect bulk semiconductor behavior. Two mechanisms can lead to direct surface-bulk coupling: near-surface band bending and defect exchange with dangling bonds.

Band bending near a free surface or solid-solid interface occurs when dangling bonds in those regions exchange charge with the semiconductor bulk. This charge exchange sets up a space charge region (and associated electric field) within the semiconductor. When point defects within the semiconductor are charged, this electric field provides an electrostatic coupling mechanism between the surface or interface and the bulk defects (Dev *et al.* 2003). For a semiconductor such as silicon, for which surfaces and interfaces typically support Fermi level pinning near the middle of the band gap, the direction of the electric field typically repels charged defects within the bulk. At high semiconductor doping levels, the electric field within the space charge region is so strong that field-induced drift dominates diffusion of the defects. Thus, the ability of the surface or interface to absorb defects from deep within the bulk is greatly diminished. However, the variation in

Fermi level near the surface or interface can also change the average charge state of charged defects in that vicinity, leading to complex effects such as the pileup of implanted dopants (Jung *et al.* 2005). The degree of band bending can, in principle, be controlled through adsorption at a free surface (Rosenwaks *et al.* 2004) and ion bombardment at a solid-solid interface (Dev *et al.* 2003; Rosenwaks *et al.* 2004).

Defect exchange with dangling bonds at a surface also provides a method to withdraw defects from the underlying semiconductor bulk (Kirichenko *et al.* 2004). An atomically clean surface can annihilate interstitial atoms by simple addition of the interstitials to dangling bonds. But if the surface is decorated with a strongly bound adsorbed species, defect annihilation requires the insertion of interstitials into existing bonds. This process should have a higher activation barrier and a correspondingly reduced probability of occurrence (Vaidyanathan *et al.* 2006a). Such effects have been demonstrated recently in silicon implanted with silicon isotopes (Seebauer *et al.* 2006) and arsenic (Vaidyanathan *et al.* 2006a). The latter case points to the possibility of creating very shallow p-n junctions with exceptionally high levels of electrically active dopant.

This exchange mechanism can also inject defects into the semiconductor whose defect concentration is below that indicated by thermodynamics. Seebauer *et al.* recently showed that point defect concentrations as deep as 0.5 μm within a semiconductor can be controlled over several orders of magnitude through manipulation of surface chemical state through gas adsorption (Seebauer *et al.* 2006).

2.7 Non-Thermally Stimulated Defect Charging and Formation

The creation of defects in particular charge states can be stimulated non-thermally either by photostimulation or (in a near-surface region) by ion bombardment. For the most part, such phenomena represent largely uncharted territory. However, some important underlying physics have been uncovered, especially in recent years.

2.7.1 Photostimulation

Photostimulation changes the steady-state concentrations of charge carriers, which in turn can alter the average charge state of defects that are present. Such effects can propagate through into phenomena such as defect diffusion as described in Chap. 7. A non-equilibrium steady-state model can be formulated (Kwok 2007) to describe the electronic occupation of defect levels under photostimulation. The model is based on Simmons and Taylor (1971) who extend Shockley–Read statistics (Shockley and Read 1952) from the case of one distinct defect level to an arbitrary distribution of levels.

In brief, the electron occupancy of any defect level is determined by the interplay of four electron transitions between the defect level, the conduction band, and

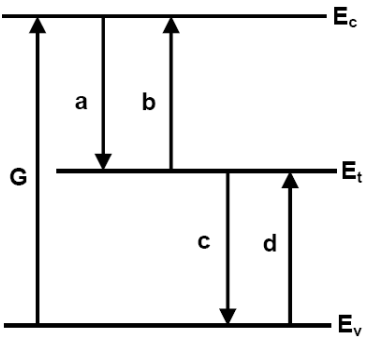

Fig. 2.7 Electronic transitions under photo-stimulation between the conduction band (a and b), valence band (c and d), and a defect level at energy E_t.

the valence band, as shown in Fig. 2.7. The probability of occupation f of the ith defect level under photostimulation can be calculated by solving the mass balance equations for electrons and holes,

$$\frac{dn}{dt} = G - \sum_i \nu_n \sigma_n^i n N_t^i(E_t^i)[1 - f(E_t^i)] + \sum_i e_n^i N_t^i(E_t^i) f(E_t^i) \tag{2.84}$$

where

$$e_n = \nu_n \sigma_n N_c \exp[(E_t - E_c)/kT] \tag{2.85}$$

$$e_p = \nu_p \sigma_p N_v \exp[(E_v - E_t)/kT] \tag{2.86}$$

with N_t and E_t denoting respectively the defect density and the defect level. E_c and E_v are respectively the conduction band minimum and the valence band maximum, with N_c and N_v denoting the corresponding density of states. The quantity v is the thermal velocity, σ is the capture cross section, where the subscripts "n" and "p" denotes respectively electrons and holes. $G(x)$ is the photo-generation rate of electron-hole pairs at a particular depth x (Blood and Orton 1992). Under steady-state conditions, $dn/dt = dp/dt = 0$. Moreover, the occupancy of any defect level E_t is constant, therefore,

$$\begin{aligned} &\nu_n \sigma_n n N_t(E_t)[1 - f(E_t)] - e_n N_t(E_t) f(E_t) - \ldots \\ &\quad \nu_p \sigma_p p N_t(E_t) f(E_t) + e_p N_t(E_t)[1 - f(E_t)] = 0. \end{aligned} \tag{2.87}$$

The unknowns include n, p, and f of each defect level. Satisfaction of the charge neutrality condition then gives a unique solution.

2.7.2 Ion-Defect Interactions

Ion bombardment, even at energies as low as about 10 eV, can also stimulate defect formation in semiconductors. Such phenomena play a key role in determining material properties in applications such as plasma enhanced deposition, reactive

ion etching, ion beam assisted deposition, and ion implantation. Adjustment of the solid temperature during ion exposure affects the results; such effects have been well studied in the context of plasma etching (Wong-Leung *et al.* 2001; Tsujimoto *et al.* 1991; Gregus *et al.* 1993), ion implantation (Nitta *et al.* 2002; Turkot *et al.* 1995; Shoji *et al.* 1992), and beam-assisted deposition (Nastasi *et al.* 1996).

Ions act mainly by knocking atoms out of their lattice sites on the surface or in the bulk, thereby creating surface or bulk vacancies as well as adatoms or interstitials. In principle, defect charging can affect the dynamics of such processes. For example, consider a case wherein a vacancy or interstitial produced by ion impact can assume different charge states depending upon the position of the Fermi energy. If the defect can ionize rapidly (even during the impact), it is reasonable to suppose that parameters such as the threshold energy for defect formation might depend upon the charge state the defect finally assumes, and thereby indirectly upon the Fermi energy. Consequently, variations in Fermi level would show up in the defect formation probability. Additionally, Wang and Seebauer indicate that some of the excess defects formed via ion-stimulation can either annihilate or form bound complexes at a rate influenced by electrostatic forces (2005). In this instance, charged defect concentration would be affected not by formation dynamics, but rather by the kinetics of annihilation with preexisting defects.

Such effects could be quite pronounced at low incident ion energies, or at higher energies near the final stopping point of the ion when most of the incident energy has been lost to the solid. These effects are incompletely explored and likely to be complicated. For example, measurements of beam-assisted deposition (Dodson 1991; Kuronen *et al.* 1999; Rabalais *et al.* 1996; Lee *et al.* 1998a; Marton *et al.* 1998) and surface diffusion (Ditchfield and Seebauer 1999, 2001) have suggested that solid temperature may directly affect the dynamics of defect formation when ion energies fall below about 100 eV. This effect is surprising, given the fact that thermal energies of the target atoms in the solid are only a few tens of meV. Wang and Seebauer have outlined a mechanism explaining such effects (2005) based on measurements of surface diffusion. However, molecular dynamics simulations suggest that the effects operate for a wide variety of crystalline solids and defect types, both on the surface and in the bulk (Wang and Seebauer 2002). Such effects could ultimately be exploited in a variety of applications, such as modulating the dynamics of defect formation near the *pn* junction of semiconductor devices during the ion implantation of dopants. Judicious tuning of temperature and ion energy may also enable the selection of specific defect formation or sputtering processes during ion beam-assisted deposition and reactive etching.

References

Bak T, Nowotny J, Rekas M *et al.* (2003) J Phys Chem Solids 64: 1043–56
Ball JA, Grimes RW, Price DW (2005) Modell Simul Mater Sci Eng 13: 1353–1363
Baumberger F, Greber T, Osterwalder J (2000) Phys Rev B: Condens Matter 62: 15431–4

Beke DL, Kaganovskii YS (1995) Mater Sci Eng, B B32: 185–199
Belova IV, Murch GE (1999) Philos Mag A 79: 1509–15
Bernstein N, Mehl MJ, Papaconstantopoulos DA *et al.* (2000) Phys Rev B: Condens Matter 62: 4477–4487
Binh VT, Melinon P (1985) Surf Sci 161: 234–244
Blakely JM (1973) *Introduction to the Properties of Crystal Surfaces,* New York, Pergamon Press
Blood P, Orton JW (1992) *The Electrical Characterization of Semiconductors: Majority Carriers and Electron States,* London, Academic Press
Bonzel HP (1973) *Structure and Properties of Metal Surfaces,* Tokyo, Maruzen Co., Ltd
Bourgoin JC, Lannoo M (1981) *Point Defects in Semiconductors,* Berlin, Springer
Bracht H, Haller EE (2000) Phys Rev Lett 85: 4835
Breeman M, Boerma DO (1992) Surf Sci 269–270: 224–8
Brouwer G (1954) Phillips Res Rep 9: 366–376
Bube RH (1992) *Photoelectric Properties for Semiconductors,* Cambridge, Cambridge University Press
Cai J (1999) Phys Stat Sol (b) 212: 9–18
Casey HC, Jr., Miller BI, Pinkas E (1973) J Appl Phys 44: 1281–7
Chang CM, Wei CM, Chen SP (1996) Phys Rev B: Condens Matter 54: 17083–96
David L, Bernard J, Orrit M *et al.* (1989) Chem Phys 132: 31–39
Dev K, Seebauer EG (2003) Phys Rev B: Condens Matter 67: 035312
Dev K, Jung MYL, Gunawan R *et al.* (2003) Phys Rev B: Condens Matter 68: 195311
Diebold U (2003) Appl Phys A 76: 681–7
Ditchfield R, Seebauer EG (1999) Phys Rev Lett 82: 1185
Ditchfield R, Seebauer EG (2001) Phys Rev B: Condens Matter 63: 125317–1
Dobson TW, Wager JF (1989) J Appl Phys 66: 1997–2001
Dodson BW (1991) Nucl Instrum Methods Phys Res, Sect B 59–60: 481
Doi T, Ichikawa M, Hosoki S *et al.* (1995) Surf Sci 343: 24–30
Ehrlich G, Hudda FG (1966) J Chem Phys 44: 1039–1040
El-Hdiy A, Salace G, Petit C *et al.* (1993) J Appl Phys 74: 1124
Erhart P, Albe K (2006) Appl Phys Lett 88: 201918
Fahey PM, Griffin PB, Plummer JD (1989) Rev Mod Phys 61: 289–384
Flynn CP (1968) Phys Rev 171: 682–698
Fu-Hsing L (1999) Comput Mater Sci 14: 48–55
Fukutani K (1993) Surf Sci 281: 285–295
Gomer R (1996) *Surface Diffusion,* London, Plenum Press
Gregus JA, Vernon MF, Gottscho RA *et al.* (1993) Plasma Chem Plasma Process 13: 521–37
Gunawan R, Jung MYL, Braatz RD *et al.* (2003) J Electrochem Soc 150: 758–65
Hansen DA, Halbach MR, Seebauer EG (1996) J Chem Phys 104: 7338
Heidberg J, Kampshoff E, Kuehnemuth R *et al.* (1992) Surf Sci 272: 306–312
Hoshino K, Peterson NL, Wiley CL (1985) J Phys Chem Solids 46: 1397–411
Hu SM (1973) Phys Status Solidi B 60: 595–604
Jarzebski ZM (1973) *Oxide Semiconductors,* New York, Pergamon Press
Jellison GE, Jr., Modine FA (1983) Phys Rev B: Condens Matter 27: 7466–72
Jun-Liang Z, Wenqing Z, Xiao-Min L *et al.* (2006) J Phys: Condens Matter 18: 1495–508
Jung MYL, Gunawan R, Braatz RD *et al.* (2003) J Electrochem Soc 150: 838–42
Jung MYL, Gunawan R, Braatz RD *et al.* (2004a) J Electrochem Soc 151: 1–7
Jung MYL, Gunawan R, Braatz RD *et al.* (2004b) AlChE J 50: 3248–3256
Jung MYL, Kwok CTM, Braatz RD *et al.* (2005) J Appl Phys 97: 063520
Kato K (1993) J Phys: Condens Matter 5: 6387–406
Kawai T, Watanabe K (1997) Surf Sci 382: 320–325
King PDC, Veal TD, Jefferson PH *et al.* (2007) Phys Rev B: Condens Matter 75: 115312–7
Kirichenko TA, Banerjee SK, Hwang GS (2004) Phys Status Solidi B 241: 2303–2312
Kohan AF, Ceder G, Morgan D *et al.* (2000) Phys Rev B: Condens Matter 61: 15019–27

Kotlyarevsky MB, Rogozin IV, Marakhovsky AV (2005) in Zinc Oxide – A Material for Micro- and Optoelectronic Applications Nickel N & Terukov E (Eds.) Netherlands, Springer
Kroger FA, Vink HJ (1958) J Phys Chem Solids 5: 208–223
Kuball M, Kelly MK, Cardona M *et al.* (1994) Phys Rev B: Condens Matter 49: 16569
Kudriavtsev Y, Villegas A, Godines A *et al.* (2005) Appl Surf Sci 239: 273–278
Kumeda Y, Wales DJ, Munro LJ (2001) Chem Phys Lett 341: 185–194
Kuronen A, Tarus J, Nordlund K (1999) Nucl Instrum Methods Phys Res, Sect B 153: 209–12
Kwok CTM (2007) Advanced methods for defect engineering in silicon Ph.D. diss. University of Illinois at Urbana-Champaign
Kyuno K, Cahill DG, Averback RS *et al.* (1999) Phys Rev Lett 83: 4788–91
Laidler KJ (1980) *Chemical Kinetics,* New York, Wiley
Landsberg PT (1991) *Recombination in Semiconductors,* Cambridge, Cambridge University Press
Lautenschlager P, Garriga M, Vina L *et al.* (1987) Phys Rev B: Condens Matter 36: 4821–30
Lee SM, Fell CJ, Marton D *et al.* (1998a) J Appl Phys 83: 5217
Lee WC, Lee SG, Chang KJ (1998b) J Phys: Condens Matter 10: 995–1002
Macdonald D, Cuevas A (2003) Phys Rev B: Condens Matter 67: 075203
Marton D, Boyd KJ, Rabalais JW (1998) J Vac Sci Technol, A 16: 1321
Millot F, Picard C (1988) Solid State Ionics 28–30: 1344–1348
Mills B, Douglas P, Leak GM (1969) Trans Met Soc AIME 245: 1291–1296
Munro LJ, Wales DJ (1999) Phys Rev B: Condens Matter 59: 3969–3980
Nastasi M, Mayer JW, Hirvonen JK (1996) *Ion-Solid Interactions: Fundamentals and Applications,* New York, Cambridge University Press
Nelson JS, Schultz PA, Wright AF (1998) Appl Phys Lett 73: 247–9
Ness H, Fisher AJ, Briggs GAD (1997a) Surf Sci 380: L479–L484
Ness H, Fisher AJ, Briggs GAD (1997b) Surf Sci 380: L479–L484
Nitta N, Taniwaki M, Suzuki T *et al.* (2002) Materials Transactions 43: 674–80
Oba F, Nishitani SR, Isotani S *et al.* (2001) J Appl Phys 90: 824–8
Pichler P (2004) *Intrinsic Point Defects, Impurities, and their Diffusion in Silicon,* New York, Springer-Verlag/Wein
Plummer EW, Rhodin TN (1968) J Chem Phys 49: 3479–3496
Queisser HJ, Haller EE (1998) Science 281: 945–50
Rabalais JW, Al-Bayati AH, Boyd KJ *et al.* (1996) Phys Rev B: Condens Matter 53: 10781–92
Rice SA (1958) Phys Rev 112: 804–811
Rosenwaks Y, Shikler R, Glatzel T *et al.* (2004) Phys Rev B: Condens Matter 70: 085320
Sahli B, Fichtner W (2005) Phys Rev B: Condens Matter 72: 245210
Saranin AA, Numata T, Kubo O *et al.* (1997) Phys Rev B: Condens Matter 56: 7449–7454
Sasaki K, Maier J (1999a) J Appl Phys 86: 5434–5443
Sasaki K, Maier J (1999b) J Appl Phys 86: 5422–5433
Schmidt J, Berge C, Aberle AG (1998) Appl Phys Lett 73: 2167
Schultz PA (2006) Phys Rev Lett 96: 246401
Seebauer EG, Allen CE (1995) Prog Surf Sci 49: 265–330
Seebauer EG, Jung MYL (2001) in Landolt-Bornstein Numerical Data and Functional Relationships: Adsorbed Layers on Surfaces Bonzel Hp (Eds.) New York, Springer Verlag
Seebauer EG, Dev K, Jung MYL *et al.* (2006) Phys Rev Lett 97: 055503
Seeger A, Chik KP (1968) Phys Status Solidi B 29: 455–542
Sharma BL (1990) Diffus Defect Data, Pt A 70/71: 1–102
Sheinkman MK, Kashirina NI, Kislyuk VV (1998) Electric field-caused redistribution of mobile charged donors in semiconductors. 1:89–92 (IEEE, Sinaia, Romania, 1998)
Shockley W, Read JWT (1952) Phys Rev 87: 823–842
Shoji K, Fukami A, Nagano T *et al.* (1992) Appl Phys Lett 60: 451–3
Simmons JG, Taylor GW (1971) Physical Review B (Solid State) 4: 502–11
Stolk PA, Gossmann HJ, Eaglesham DJ *et al.* (1997) J Appl Phys 81: 6031
Swalin RA (1962) J Phys Chem Solids 23: 154–156
Thurmond CD (1975) J Electrochem Soc 122: 1133–1141

Tomlins GW, Routbort JL, Mason TO (1998) J Am Ceram Soc 81: 869–876
Tsoga A, Nikolopoulos P (1994) J Am Ceram Soc 77: 954–960
Tsujimoto K, Okudaira S, Tachi S (1991) Jpn J Appl Phys 30: 3319–3326
Tuomisto F (2005) Vacancy defects in semiconductor materials for opto and spin electronics Ph.D. diss. Helsinki University of Technology
Turkot BA, Forbes DV, Robertson IM *et al.* (1995) J Appl Phys 78: 97–103
Ural A, Griffin PB, Plummer JD (1999) Phys Rev Lett 83: 3454–3457
Ural A, Griffin PB, Plummer JD (2000) Phys Rev Lett 85: 4836–4836
Vaidyanathan R, Seebauer EG, Graoui H *et al.* (2006a) Appl Phys Lett 89: 152114
Vaidyanathan R, Jung MYL, Braatz RD *et al.* (2006b) AlChE J 52: 366–370
Van Vechten JA (1980) in Handbook on Semiconductors Keller Sp (Eds.) New York, North-Holland
Van Vechten JA, Thurmond CD (1976a) Phys Rev B: Condens Matter 14: 3539–50
Van Vechten JA, Thurmond CD (1976b) Phys Rev B: Condens Matter 14: 3551–7
Varshni YP (1967) Physica 34: 149–154
Vineyard GH (1957) J Phys Chem Solids 3: 121–127
Vitomirov IM, Waddill GD, Aldao CM *et al.* (1989) Phys Rev B: Condens Matter 40: 3483
Wang Z, Seebauer EG (2002) Phys Rev B: Condens Matter 66: 205409–1
Wang Z, Seebauer EG (2005) Phys Rev Lett 95: 015501
Watkins GD (1967) Phys Rev 155: 802–815
Watkins GD (1975) EPR studies of the lattice vacancy and low-temperature damage processes in silicon. In: Lattice Defects in Semiconductors, 1974 1–22 (Inst. Phys, Freiburg, West Germany, 1975)
Watkins GD (1986) Mater Sci Forum 10–12: 953–60
Watkins GD, Troxell JR, Chatterjee AP (1979) Vacancies and interstitials in silicon. In: International Conference on Defects and Radiation Effects in Semiconductors 16–30 (Inst. Phys, Nice, France, 1979)
Wong-Leung J, Jagadish C, Conway MJ *et al.* (2001) J Appl Phys 89: 2556–2559
Yagi K, Yamanaka A, Yamaguchi H (1993) Surf Sci 283: 300–308
Zener C (1951) J Appl Phys 22: 372–375

http://www.springer.com/978-1-84882-058-6

Charged Semiconductor Defects
Structure, Thermodynamics and Diffusion
Seebauer, E.G.; Kratzer, M.C.
2009, XIV, 298 p., Hardcover
ISBN: 978-1-84882-058-6